Liquid Crystals
Publication details, including instructions for authors and subscription information:
http://www.informaworld.com/smpp/title~content=t713926090

Study of the biaxiality in the nematic phase of liquid crystals in terms of orientational order parameters by infrared spectroscopy

A. Kocot[ab]; J. K. Vij[a]
[a] Department of Electronic and Electrical Engineering, School of Engineering, Trinity College, University of Dublin, Dublin, Ireland [b] Institute of Physics, Silesian University, Katowice, Poland

Online publication date: 06 July 2010

To cite this Article Kocot, A. and Vij, J. K.(2010) 'Study of the biaxiality in the nematic phase of liquid crystals in terms of orientational order parameters by infrared spectroscopy', Liquid Crystals, 37: 6, 653 — 667
To link to this Article: DOI: 10.1080/02678292.2010.488372
URL: http://dx.doi.org/10.1080/02678292.2010.488372

Liquid Crystals,
Vol. 37, Nos. 6–7, June–July 2010, 653–667

Taylor & Francis
Taylor & Francis Group

INVITED ARTICLE

Study of the biaxiality in the nematic phase of liquid crystals in terms of orientational order parameters by infrared spectroscopy

A. Kocot[a,b] and J.K. Vij[a*]

[a]*Department of Electronic and Electrical Engineering, School of Engineering, Trinity College, University of Dublin, Dublin, Ireland;* [b]*Institute of Physics, Silesian University, Katowice, Poland*

(*Received 1 February 2010; accepted 18 April 2010*)

The observation and quantification of the biaxiality in the nematic phase of thermotropic liquid crystals is one of the topical problems in the science of liquid crystals. The biaxiality in the refractive index and/or relative permittivity, both constituting tensors of the second rank, are expressed in terms of the four scalar order parameters S, D, P and C and the relevant molecular quantities. In this paper we review the theory of determining these order parameters using polarised infrared spectroscopy and present the method that we have developed in obtaining results for the order parameters of tetrapodes (with symmetrical and asymmetrical mesogens) and tripodes with symmetrical mesogens. In the tetrapodes, four mesogens are linked through the siloxane chains to the central Si atom. In the tripode, three mesogens are linked to a benzene ring via the oxygen atom through the siloxane spacers. In the first case a platelet-like structure is formed where the major director corresponds to the highest refractive index. A disc-like structure is formed for a tetrapode with symmetrical mesogens and for a tripode. The order parameters are calculated in the framework of the quasi-flat platelets. For the discotic-like structure, the major director corresponds to the lowest of the three refractive indices. For the three cases, the compounds are shown to exhibit a biaxial nematic phase. Biaxiality in the refractive indices is expressed in terms of the biaxial order parameters. A comparison of the results on the I–N_U and N_U–N_B transitions for tetrapodes compare favourably with the predictions from the mean field models of de Gennes, Virga and his co-workers.

Keywords: biaxial nematic phase; siloxane tetrapodes; siloxane tripodes; polarised infrared spectroscopy

1. Introduction

Liquid crystals are composed of strongly anisotropic molecules which are generally biaxial. Most of the commonly observed phases are nematics and smectics; of the smectics, SmA and SmC are the most common and simpler structures. However, both the nematic and SmA phases are normally uniaxial because the molecular rotations are approximately cylindrically symmetric, leading in general to such a phase. In both nematic and smectic phases, no long-range orientational order is present, as in the isotropic (I) phase, but molecules on the average are parallel to each other. The preferred direction of orientation is called the director. Alfred Saupe expressed the temperature dependence of the orientational order parameter of the nematic phase by ingeniously calculating the mean-field potential, famously known as the Maier–Saupe potential, in terms of the scalar orientational order parameter, *S*, and the relative orientation of the molecules from the nematic director [1]. This work formed the basis of Alfred Saupe's PhD thesis. Bisi *et al.* [2] have rightly suggested that this *potential* be henceforth called the *molecular field potential*, due to its molecular nature and furthermore its distinction from the mean-field phenomenological model of Landau and de Gennes [3]. The use of an altered terminology from the mean field to the molecular field is thus a fitting tribute to the many seminal works of Alfred Saupe. As already pointed out, the nematic phase is often comprised of molecules which do not generally have infinite rotational axis and thus lack the perfect cylindrical symmetry $D_{\infty h}$. In such cases the symmetry might be consistent with D_{2h} where the directors *l*, *m* and *n* are associated with the preferred orientations of the three symmetry axes of the orthorhombic molecular block. Freiser [4] generalised the Maier–Saupe molecular field theory by including two second-rank tensor order parameters for a lower symmetry system. These tensor order parameters were expressed in terms of the three mutually orthogonal unit vectors in the molecular frame. These tensors can be diagonalised using a frame that coincides with the directors of a biaxial nematic phase. This diagonalisation gives rise to the four Straley scalar order parameters [5], to be discussed later. Thus a biaxial nematic phase, predicted on theoretical grounds through a simple extension of the Maier–Saupe potential for a lower symmetry system by Freiser in 1970 is realisable. The biaxial phase has two optic axes, though not coincident

*Corresponding author. Email: jvij@tcd.ie

ISSN 0267-8292 print/ISSN 1366-5855 online

DOI: 10.1080/02678292.2010.488372
http://www.informaworld.com

with any of the major or minor directors, along which linearly polarised light can travel with its state of polarisation unaltered by its passage through the material. This phase arises from a second order phase transition from the uniaxial, N_U, to biaxial, N_B, phase at a temperature lower than the isotropic to uniaxial nematic (I–N) transition temperature. The prediction led to a considerable flurry in both theoretical and experimental work in the literature. Ten years later in 1980, Yu and Saupe discovered the first biaxial nematic phase in a lyotropic liquid crystal sandwiched between a uniaxial positive and a uniaxial negative nematic phase in a system composed of relatively large micelles [6]. Since this seminal experimental discovery, a number of studies on biaxiality, especially in thermotropic nematics, have appeared in the literature. This area of liquid crystal research continues to attract considerable interest due to the technological importance of its potential for producing fast electro-optic devices and displays, while at the same time it is highly debated and scientifically challenging [7–16]. Historically, a number of compounds claimed initially to form a thermotropic biaxial nematic phase, when re-examined by other techniques and or measurements repeated by other authors, were not unambiguously proven to exhibit a biaxial nematic phase. It is feasible that some of the compounds studied previously may have had some small biaxiality present in a part of their nematic phase, or the biaxiality may have been induced by surfaces. It is also possible that the onset of biaxiality in the nematic phase may in some cases be preceded by crystallisation. The molecular arrangement in biaxial nematics and smectics is shown in Figure 1.

SmC is biaxial mainly as a consequence of the ordering of the short molecular axes following their tilt from the layer normal. The major director is along the tilt, and one of the other two directors lies in the tilt plane and the second normal to it. However, there are no reports on the observation of biaxiality in the SmA phase, except for a system of banana-shaped molecules dispersed in an anisotropic host composed of rod-shaped molecules, where the texture is interpreted

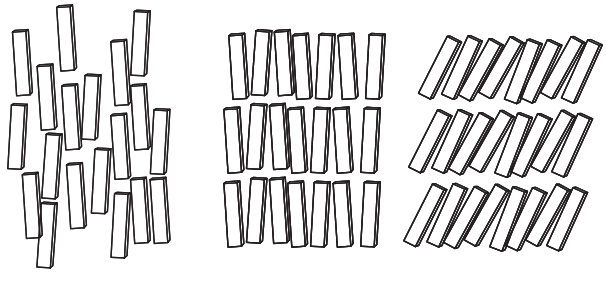

Figure 1. A schematic illustration of biaxial phases in nematic and smectic phases of thermotropic liquid crystals using board-like molecules.

in terms of a biaxial SmA phase [17]. Recently $SmAP_R$ and $SmAP_A$ phases in a few banana-shaped liquid crystal systems have been discovered [18, 19]. In these phases, the major director is directed along the layer normal, whereas the minor director (in these cases the bow director) in neighbouring layers is either randomly oriented ($SmAP_R$) or is anticlinic ($SmAP_A$). We can obtain a biaxial $SmAP_A$ polar phase by applying an in-plane electric field on assuming that these materials inherently are negative dielectric anisotropic in nature. However, biaxiality in smectics will not be discussed further in this article, except to state that the technique being outlined here is equally applicable to smectics.

The consistent pursuit of the thermotropic biaxial phase for over 30 years by liquid crystal scientists finally led to firm evidence being presented in the year 2004 for a liquid-crystalline system composed of molecules described variously as banana-like, bow, V and boomerang shaped, in which a small macroscopic biaxiality of $\eta = 0.11$ was observed using ^2H nuclear magnetic resonance (NMR) and was found to be temperature insensitive [20]. The NMR technique, as pointed out by Luckhurst [21], is extremely powerful for confirming nematic biaxiality, since the sample is studied in the bulk and furthermore its directors are not required to be aligned. The spontaneous biaxiality was confirmed independently by Acharya *et al.* [22], who showed through X-ray studies the orientation of the minor director from being initially parallel was then directed normal to the substrate's surface on the application of an electric field. The major director was aligned using a polymer coating on one of the surfaces of the substrate. Wide-angle X-ray scattering confirmed that the orientation of the major director on the application of the field was unchanged. The holy grail of liquid crystal science as stated by Luckhurst [21, 23] had thus been found. The biaxiality was also confirmed in a side-chain liquid crystalline polymer [24]. In the same year, Merkel *et al.* reported a biaxial phase in two compounds composed of molecular tetrapodes, having symmetrical and asymmetrical mesogens [25]. In these tetrapodes, the mesogens are connected to the siloxane core through four siloxane spacers and the system was shown to form a quasi-flat platelet. In order to achieve the optimised packing of the constituents, the mesogens may be tilted in the plane of the platelet. However, the platelet of the tetrapode itself is not tilted and has orthorhombic D_{2h} symmetry. This is being confirmed experimentally using infrared (IR) polarised spectroscopy on one of the tetrapodes. Measurements on the end chains of the mesogens show that these are normal to the substrate in a homeotropic cell configuration. The biaxiality in tetrapodes was confirmed by Cruz *et al.* [26, 27] using the deuterium NMR technique, where a deuteriated probe was used to carry out the investigations. The biaxiality

was also confirmed using the technique of dynamic light scattering [28] on a compound where the central Si atom was replaced by Ge; however, the chains were still siloxanes, as before.

On the computer simulations side, much more significant progress has been made. Results of computer simulations of biaxial nematics have recently been reviewed by Berardi *et al.* [29]. In an analytical theory, Coffey *et al.* [30] have analysed the dielectric relaxation of the dipoles parallel to the director (longitudinal) in the context of the model of non-inertial rotational Brownian motion of a molecule in a molecular field potential. For uniaxial molecules in a biaxial potential, they derived simple analytical expressions for the dielectric susceptibility and relaxation times in terms of parameters characterising the biaxial molecular field potential. In the limit of the negligible biaxiality, their equation for the dielectric relaxation time reduced to that of Martin *et al.* [31] for uniaxial nematic liquid crystals. To our knowledge, a complete dielectric relaxation theory of biaxial molecules in the biaxial potential has not been advanced to date. In order to investigate experimentally and quantify the biaxiality, techniques such as NMR and IR spectroscopy, as already pointed out, need to be used. Raman spectroscopy is yet another powerful technique which has recently been exploited to find two parameters of biaxiality [32]. In this paper, we focus on the development of polarised IR spectroscopy used to determine quantitatively the scalar order parameters. We examine the relevant theory of the order parameters, then focus on to the experiments and present the results for tetrapodes and tripodes.

2. Macroscopic anisotropic properties and the orientational order parameters

Most applications of liquid crystals are based on using their anisotropic properties and their dependencies on pressure, temperature and external fields. Basically, the macroscopic anisotropic properties of liquid crystals are governed by their molecular behaviour, the alignment and the orientational order of the constituent molecules [33–36]. One of the interesting problems in the science of liquid crystals that is not fully solved is that of finding a relationship between the molecular properties and the macroscopic anisotropic properties. Molecular properties are required to be transformed to the laboratory system by using a transformation matrix with which a vector defined in the molecular system is transformed to the laboratory system. This is usually written in terms of the Euler angles, which completely define the relationship between the molecular and the laboratory frames. We can express this relationship through the microscopic tensor order parameters, provided the interactions among the molecules can be neglected. Any macroscopic anisotropic property (for example, dielectric permittivity, refractive index, magnetic susceptibility) can be determined if only a set of the order parameters and the corresponding molecular properties are known. A Physical quantity such as the relative permittivity described by a second rank tensor can thus be expressed by a set of four scalar order parameters and the corresponding molecular properties. The orientational molecular order parameters are defined by the three diagonal Saupe ordering matrices [33], one for each of the three axes, $i = X, Y, Z$:

$$S^{ii}_{\alpha\beta} = \left\langle \frac{1}{2}\left(3l_{i,\alpha}l_{i,\beta} - \delta_{\alpha\beta}\right)\right\rangle, \qquad (1)$$

where $\alpha, \beta = x, y, z$; $l_{i,\alpha}$ is the cosine of the angle between the molecular axes α and the laboratory or the phase axes i. Similarly $l_{i,\beta}$ is the cosine of the angle between the molecular axes β and the phase axes, i. $\delta_{\alpha\beta}$ is the Kronecker delta, for $\alpha = \beta$; $\delta_{\alpha\beta} = 1$ and for $\alpha \neq \beta$; $\delta_{\alpha\beta} = 0$. From Equation (1), each i has three elements of S. Figure 2 shows the mutually perpendicular phase (X, Y, Z) and the molecular (x, y, z) axes and their relative orientations are given in terms of the Euler angles.

In a uniaxial phase, the ordering of the molecular long axes is described by the usual S parameter, $S = S^{ZZ}_{zz}$, a measure of the average orientation of the molecular axes, z, with respect to the laboratory axis Z. The molecular biaxiality in a uniaxial phase is described by the biaxial order parameter,

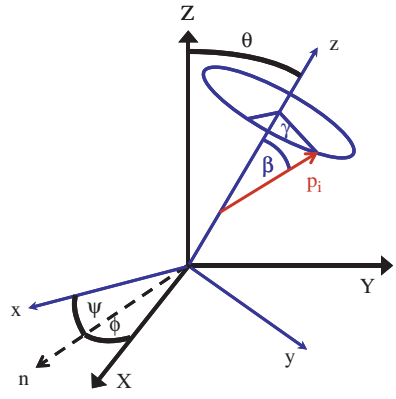

Figure 2. Schematics of the orientation of the molecular x, y and z axis system within the laboratory X, Y and Z axis system. All possible relative orientations of the two frames are described by ψ, θ, and ϕ ; θ is the polar angle, ϕ is the angle between the normal to the z–Z plane (i.e. $\boldsymbol{n}$) and the X axis. The orientation of the short axis x with respect to $\boldsymbol{n}$ is represented by ψ corresponding to the molecular rotation around z, as the axis of the highest symmetry. γ is the azimuthal angle of the transition dipole moment (the angle between the projection of the transition moment p_i on the x–y plane and the x-axis).

$D = S_{xx}^{ZZ} - S_{yy}^{ZZ}$. D is thus a measure of the difference between the orientational distribution of the two short molecular axes x and y with respect to the laboratory axis Z. If the liquid crystal phase is biaxial, then any second-rank tensor property, such as the refractive index, electric and magnetic susceptibilities, has three different principal components. The phase biaxiality is given by the order parameter, $P = S_{zz}^{XX} - S_{zz}^{YY}$; P is a measure of the difference in the probabilities of finding the z molecular axis along the X and Y directions of the laboratory system. For describing the molecular biaxiality in a biaxial phase, another biaxial order parameter is introduced, $C = D' - D'' = (S_{xx}^{XX} - S_{yy}^{XX}) - (S_{xx}^{YY} - S_{yy}^{YY})$, a difference in the distribution of the x and y axes of the molecular system with respect to the X and Y axes of the laboratory system, respectively. On using the definitions of the order parameters as expressed by the Saupe ordering matrices [33] through Equation (1), we find

$$\begin{aligned} S &= S_{zz}^{ZZ} = \frac{1}{2}\left\langle (3l_{Z,z}^2 - 1)\right\rangle, \\ D &= S_{xx}^{ZZ} - S_{yy}^{ZZ} = \frac{3}{2}\left\langle (l_{Z,x}^2 - l_{Z,y}^2)\right\rangle, \\ P &= S_{zz}^{XX} - S_{zz}^{YY} = \frac{3}{2}\left\langle (l_{X,z}^2 - l_{Y,z}^2)\right\rangle, \\ C &= (S_{xx}^{XX} - S_{yy}^{XX}) - (S_{xx}^{YY} - S_{yy}^{YY}), \\ &= \frac{3}{2}\left\langle [(l_{X,x}^2 - l_{X,y}^2) - (l_{Y,x}^2 - l_{Y,y}^2)]\right\rangle. \end{aligned} \tag{2}$$

The projection of a unit vector, directed along α, to the β axis is given by $l_{\alpha,\beta}$. On using the coordinate system given in Figure 2, the set of Equations (2) leads to

$$\begin{aligned} S &= \frac{1}{2}\langle (3\cos^2\theta - 1)\rangle, \\ D &= \frac{3}{2}\langle (\sin^2\theta \cos 2\psi)\rangle, \\ P &= \frac{3}{2}\langle (\sin^2\theta \ \cos 2\phi)\rangle, \\ C &= \frac{3}{2}\langle [(1 + \cos^2\theta)\cos 2\phi \cos 2\psi \\ &\quad -2\cos\theta \sin 2\phi \sin 2\psi]\rangle. \end{aligned} \tag{3}$$

In the first case, if the molecular rotation around its molecular long axis is free, i.e. when the molecules are rod-shaped or any orientation around its molecular z-axis (the axis of highest symmetry) is equally probable, then $\langle \cos 2\psi = 0\rangle$ and hence D is zero. In the second case, if the molecules have equal probability distributions around the laboratory X and Y axes, which means that the thermal fluctuations of the long molecular axis in both X and Y directions are equally probable, then $\langle \cos 2\phi\rangle = 0$, making $P = 0$. If both conditions are satisfied then $D = P = C = 0$. P represents the anisotropic thermal fluctuations of the long molecular axes of the constituent molecules with cylindrical symmetric rotation, and it therefore represents the phase biaxiality for uniaxial molecules. The order parameter C corresponds in a complicated way to the biased rotation around the long molecular axis. The order parameters C and P defined by the Saupe ordering matrices [33] differ from those given by Straley [5] due to a difference in their definitions. We can easily find

$$\begin{aligned} C_{\text{Saupe}} &= 3(C_{\text{Straley}} \equiv \text{V}) \\ \text{and} \\ P_{\text{Saupe}} &= \frac{3}{2}(P_{\text{Straley}} \equiv \text{T}). \end{aligned} \tag{4}$$

The S and D parameters defined by Saupe [33] and Straley (S and U) [5] are the same. Straley denoted the biaxial parameters as S, T, U and V. These are related to Saupe's S, P, D and C as given here.

3. Polarised infrared spectroscopy

Polarised IR spectroscopy is a very powerful and a valuable technique for investigating systems with an unusual molecular structure such as those in biaxial nematics and smectic liquid crystals. The polariser is rotated to vary the angle of polarisation and the spectra are recorded as a function of this angle. This is to test the symmetry of the phase. Here we present results for only two angles; one gives the maximum absorbance and the second position is adjusted at right angles to it. The use of IR spectroscopy for the study of liquid crystals was initiated in the laboratory of Glenn Brown in the mid 1960s [37], where expressions for IR dichroism in terms of the order parameter were established, though a simple expression for the IR dichroism in terms of S had already been worked out by Maier and Saupe [38]. Since the 1970s, however, the technique has been rather sparingly used in the literature. Nevertheless, IR spectroscopy itself is widely used both in industry and in the scientific literature as a fingerprint of vibrational bands of molecules for material characterisation, and for examining the behaviour of molecular conformations [39]. A study of the alignment of discotics and the investigation of their order parameter(s) has been made using polarised IR spectroscopy [40, 41]. Works on the relationship between the dependencies of absorbance on the angle of polarisation, and works on the distribution parameter of the carbonyl bond close to the chiral centre in the chiral smectics using polarised IR spectroscopy, have been reviewed previously [42]. We have developed the technique for determining a set of four scalar order parameters in order to express the second-rank

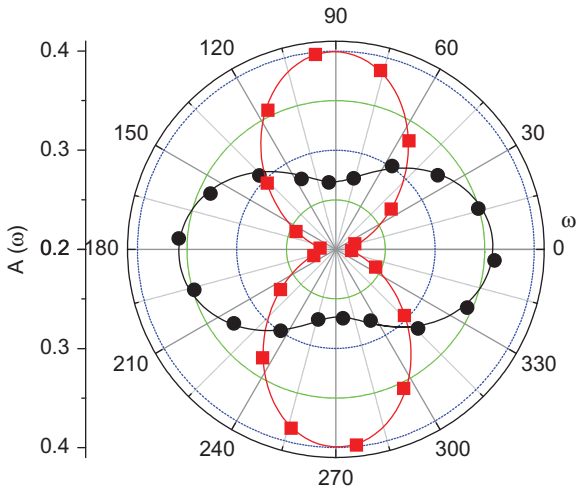

Figure 3. Polarisation angle dependence of the absorbance peak intensity $I(\omega)$: ● for the 1604 cm^{-1} band and ■ for the 762 cm^{-1} of the tetrapode *B* at 373 K in the planar configuration of the cell (colour version online).

tensorial physical property such as the refractive index or permittivity [43–45] in terms of the relevant molecular properties. The analysis presented is valid for the orthorhombic or the D_{2h} symmetry, but can be extended to monoclinic C_{2h} and triclinic C_i symmetries [46]. Normal incidence of the IR beam is being considered here. In order to probe the symmetry of the phase of the tetrapodes, we investigate the dependence of IR absorbance of a number of transition dipoles of different orientations in the molecular frame as a function of the angle of polarisation for tetrapode *B*. They all show overall D_{2h} symmetry, i.e. the absorbance profiles are oriented either at 0° or 90° with respect to each other. Figure 3 is an example for the two bands of a tetrapode: one parallel and the second normal to the core of the mesogen, phenyl stretching band at 1604 cm^{-1} and phenyl C-H out of plane 762 cm^{-1} for the homeotropic aligned sample of tetrapode *B*; their maxima lie at an angle of 90 ± 2°. This shows that the principal axes in the plane of the substrate are normal to each other within the accuracy of the experiment. The third principal axis would be at right angles to the plane containing these two axes.

We discuss a detailed quantitative relationship between the observed IR macroscopic properties and the microscopic order parameters for the second-rank order parameter tensors for the system with D_{2h} symmetry. Hild *et al.* showed that if in the calculation of the orientational order parameter, *S*, the molecular biaxial order parameter *D* in the expression was ignored, a determination of *S* alone could be subject to errors [43].

4. Infrared absorbance components

In an orientationally ordered sample, the IR absorbance components are dependent on the angle between the alignment axis and the polarisation direction of the incident light. At a microscopic level, the infrared absorption depends on the projections of a molecular transition dipole moment, μ_i, of a particular absorption band on the principal axes and the angle between the IR polarised light and the principal axes. If the effect of the molecular interactions and the local field are neglected, then the absorbance components along the principal laboratory axes can be written down in terms of the components of the dipole moment along the molecular axes. Since the components need to be averaged over all possible orientations of molecules, the averages over the products of direction cosine matrices contain the orientational order parameters. The theory has been worked out for the magnetic susceptibility [33] and we adapt the equations derived from this to IR spectroscopy. The absorbance components along the laboratory axes *X*, *Y* and *Z* are found to be

$$\begin{aligned}
A_{XX} &= A_0 - B\left[\frac{1}{3}(S-P)\left\{(\mu_i)_n^2 - \frac{1}{2}\left((\mu_i)_l^2 + (\mu_i)_m^2\right)\right\} + \frac{1}{6}(D-C)\left\{(\mu_i)_l^2 - (\mu_i)_m^2\right\}\right],\\
A_{YY} &= A_0 - B\left[\frac{1}{3}(S+P)\left\{(\mu_i)_n^2 - \frac{1}{2}\left((\mu_i)_l^2 + (\mu_i)_m^2\right)\right\} + \frac{1}{6}(D+C)\left\{(\mu_i)_l^2 - (\mu_i)_m^2\right\}\right],\\
A_{ZZ} &= A_0 + B\left[\frac{2}{3}S\left\{(\mu_i)_n^2 - \frac{1}{2}\left((\mu_i)_l^2 + (\mu_i)_m^2\right)\right\} + \frac{1}{3}D\left\{\left((\mu_i)_l^2 - (\mu_i)_m^2\right)\right\}\right],
\end{aligned} \tag{5}$$

where

$$A_0 = \frac{1}{3}(A_{XX} + A_{YY} + A_{ZZ}). \tag{6}$$

A_0 is the mean absorbance of the isotropic fluid; μ_l, μ_m, μ_n, are the components of the transition moment along the principal molecular axes l, m, n for the particular absorption band. If the correlations of the transition dipoles expressed by the Kirkwood correlation factor are neglected, then the summation rule, $B\mu^2 = A_0$, must be obeyed; here A_0 is a constant. It is more convenient to express the set of equations in terms of the direction cosines of dipolar directions; since $(\mu_i)_l = |\mu_i| l_i$, the set of Equations (5) becomes

$$
\begin{aligned}
A_{XX} &= A_0 - B(|\mu_i|)^2\left[\tfrac{1}{3}(S-P)\left\{(l_i)_n^2 - \tfrac{1}{2}\left((l_i)_l^2 + (l_i)_m^2\right)\right\} + \tfrac{1}{6}(D-C)\left\{(l_i)_l^2 - (l_i)_m^2\right\}\right],\\
A_{YY} &= A_0 - B(|\mu_i|)^2\left[\tfrac{1}{3}(S+P)\left\{(l_i)_n^2 - \tfrac{1}{2}\left((l_i)_l^2 + (l_i)_m^2\right)\right\} + \tfrac{1}{6}(D+C)\left\{(l_i)_l^2 - (l_i)_m^2\right\}\right],\\
A_{ZZ} &= A_0 + B(|\mu_i|)^2\left[\tfrac{2}{3}S\left\{(l_i)_n^2 - \tfrac{1}{2}\left((l_i)_l^2 + (l_i)_m^2\right)\right\} + \tfrac{1}{3}D\left\{\left((l_i)_l^2 - (l_i)_m^2\right)\right\}\right].
\end{aligned}
\tag{7}
$$

However, it is sometimes convenient to relate the absorbance components to the mean value of the absorbance measured in a disordered system, i.e. in the isotropic phase. A set of relations (see Equations (7)) for the absorbance can be converted into angular dependencies of the polar and azimuthal angles of the transition moment shown in Figure 2. The transition moments can have any orientation in the three-dimensional space. These result in the following set of equations

$$
\begin{aligned}
A_{XX}/A_0 &= 1 + (S-P)\left[\tfrac{3}{2}\sin^2\beta - 1\right]\\
&\quad + \tfrac{1}{2}(D-C)[\sin^2\beta\cos 2\gamma],\\
A_{YY}/A_0 &= 1 + (S+P)\left[\tfrac{3}{2}\sin^2\beta - 1\right]\\
&\quad + \tfrac{1}{2}(D+C)[\sin^2\beta\cos 2\gamma]
\end{aligned}
\tag{8}
$$

and

$$
\begin{aligned}
A_{ZZ}/A_0 &= 1 + S[2 - 3\sin^2\beta]\\
&\quad - D[\sin^2\beta\cos 2\gamma],
\end{aligned}
$$

where β is the polar angle between the transition dipole moment and the z-axis of the molecule, γ is the azimuthal angle, the angle between the projection of the transition dipole on the x–y plane and the x-axis of the molecular system shown in Figure 2. Values of β for different bands are obtained from molecular structure simulations, $\beta \sim 0^\circ$ for the phenyl band at $\sim$1608 cm^{-1}. However, in cases where the phenyl rings are separated by a carbonyl group, β varies from 6 to 10°; $\beta = 61^\circ$ for the carbonyl dipole at 1708 cm^{-1}, but it can also vary from 60 to 80° depending on the molecular structure. γ is estimated by fixing the molecular coordinate system to the geometry of the molecule, see Figure 4 for a tetrapode having longer mesogens with the symmetrical disposition of the carbonyl bonds, as is conveniently possible and it can then be easily determined. γ for a given bond and conformation is fixed since this is the azimuthal angle of the transition dipole moment in the molecular system, but its value may be different for different conformers. In a complicated system there may be two carbonyl bonds; one of these lies in the z–x plane, for which $\gamma = 0$, but the second may be at an angle to this plane and its γ needs to be estimated. Such cases are considered separately by estimating the contribution to the absorbances made by each band. In many cases the molecular simulations are helpful in finding the appropriate values of β and γ for a vibrational band of interest. If $\beta \approx 0^\circ$, the set of Equations (8) indicates that γ need not be known. Table 1 gives vibrational frequencies for a number of commonly observed bands of mesogenic molecules with their polarisations, parallel and transverse, as measured with reference to their molecular long axes.

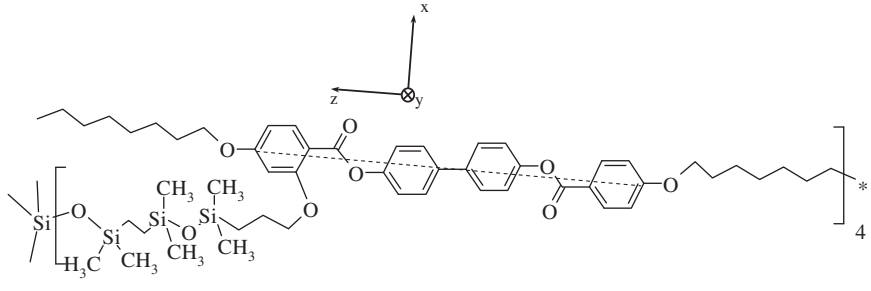

Figure 4. Structure of a conformer of siloxane tetrapode *B* and its molecular frame of reference. Each mesogen has four benzene rings with the symmetrical disposition of benzene rings. Transition temperatures are given later in Figure 6(b).

Table 1. Assignment of the vibrational bands used in liquid crystalline systems with their polarisations. The bands with wave numbers underlined are intense and commonly used.

Wavenumber cm^{-1}	Assignment	Polarisation
3040	CH stretching	∥
2956	CH_3 asymmetric stretching	⊥
2928	CH_2 asymmetric stretching	⊥
2872	CH_3 symmetric stretching	⊥
2857	CH_2 symmetric stretching	⊥
1737	C=O stretching	⊥
1606	Phenyl ring stretching	∥
1572	Phenyl ring stretching	∥
1510	Phenyl ring stretching	∥
1495	CH_3 asymmetric deformation + phenyl ring stretching	
1468	CH_2 scissoring mode	⊥
1422	CH_2 scissoring mode	⊥
1390	CH_3 in-plane symmetric deformation	
1300	Phenyl C–C in-plane deformation	∥
1270	Si–CH_3 symmetric deformation	
1254	Ph–O–C stretching	∥
1198	Phenyl C–H in-plane deformation	∥
1164	Phenyl C–H in-plane deformation + C–C–C skeleton vibration	∥
1134	Phenyl C–H in-plane deformation	∥
1069	Si–O–Si stretching	∥
1053	Al–O–C asymmetric stretching	∥
1005	Phenyl C–C in-plane deformation	∥
868	CH_2 rocking mode + phenyl C–H out-of-plane	⊥
836	C–O–C symmetric stretching + Si–C symmetric stretching	⊥
793	Si–CH_3 rocking	⊥
763	Phenyl C–H out-of-plane	⊥
656	Phenyl C–C in-plane deformation	∥

Measurements made in the planar configuration give A_{YY} and A_{ZZ}. For the cell in the homeotropic configuration, two absorbance components, A_{XX}, and one out of the other two components, A_{YY} (or A_{ZZ}), are measured. The latter needs to coincide with either of the two components measured in the planar configuration, and this decides as to which of the two components it corresponds. In this way we have two equations for each transition dipole moment preselected depending on the molecular structure under investigation. The two appropriate dominant vibrational bands for known values of β are picked from a given molecular structure. For calculating the order parameters for the mesogen, the two bands selected are usually the phenyl stretching vibration ~1160 cm^{-1} or at ~1608 cm^{-1} and the carbonyl stretching band at ~1738 cm^{-1}. The azimuthal angle, γ, is found using the method given later. In many cases $\gamma \sim 0°$ or $\pm$ 180°, if the transition moment lies in the x–z plane. Since γ is the angle between the projection of the transition moment, on the y–x plane, and the x-axis and if the projection is parallel or anti-parallel to the x-axis, then $\gamma = 0°$ (180°). In either case, $\cos 2\gamma = 1$. If $\gamma = 90°$ or (–90°), i.e. the projection is along or against the y-axis, $\cos 2\gamma = -1$ for both positive and negative γ. Intermediate values of γ are also possible. On the other hand, if the components of the transition moment along the three axes are known, then a set of Equations (8) can be used to find the set of scalar order parameters. A_0 is determined as the total absorbance above the N–I transition temperature,

$$\frac{A_{XX} + A_{YY}}{2A_0} = 1 + S\left(\frac{3}{2}\sin^2\beta - 1\right) + \frac{D}{2}\sin^2\beta\cos 2\gamma,$$
$$\frac{A_{YY} - A_{XX}}{2A_0} = P\left(\frac{3}{2}\sin^2\beta - 1\right) + \frac{C}{2}\sin^2\beta\cos 2\gamma. \quad (9)$$

In order to find the set of four scalar order parameters, we again need to select at least two appropriate dominant vibrational bands with known values of β. γ is determined as discussed previously. We can thus find the four scalar order parameters as average values over the four mesogens, for the chains and for the spacers of a tetrapode.

5. Experimental method

The schematic of the experimental set up is shown in Figure 5. The sample cell is mounted within a heating/

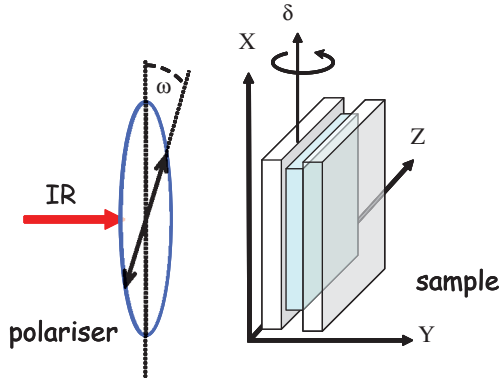

Figure 5. A schematic of the measurement system is shown. Cell of KBr/ZnSe windows containing the sample is mounted on the heating/cooling stage and the IR beam is incident normally. The cell can be rotated along the normal to the direction of incident IR beam as shown, by a motor attachment. The polariser mounted on a special mount can be rotated automatically with an angular accuracy of ± 0.1°. For the planar homogeneously aligned sample both A_{XX} and A_{ZZ} can be measured. For the homeotropic sample, A_{XX} and A_{YY} are measured; axes X, Y and Z of the laboratory system are shown for the homeotropic configuration, with Z more or less lying along the director in both cases. For the homeotropic alignment, the laboratory axes Y and Z are rotated around X by an angle of 90°.

cooling stage. The homogeneously planar-oriented sample was obtained by coating KBr/ZnSe windows with a polymer solution coating. In order to obtain homogeneous orientation of the director on the sample windows, these were spin-coated with a 0.2% solution of nylon 6/6 in methanol, dried at ~100°C for about 30 min, following which one of the two windows was rubbed in a specific direction. Mylar foil was used as a spacer, and the thickness of the cells fabricated was determined by the measurements of the interference fringes. The sample for the IR study was aligned in between the optically polished KBr/ZnSe windows. The quality of the alignment has been tested using polarising microscopy. The texture of the sample was monitored using a polarising microscope that was used for characterising the phase prior to its investigation by polarised IR spectroscopy. The optical axis of the sample stays fixed parallel to the rubbing direction and a reasonably high contrast ratio is observed. Only ZnSe windows are transparent to both the visible and IR. Homeotropic alignment was obtained by coating KBr/ZnSe windows with a carboxylatochromium complexes (chromolane) 1% solution in iso-propanol. The solution was spin coated at a speed of ~2000 rev/min for 100 s and then the substrate was baked at 150°C. Alternatively, we have also spin coated the KBr/ZnSe windows with AL60702 polymer solution (JSR Corp. Japan) obtained through Samsung, Korea, for the homeotropic alignment. In some cases this is a better aligning agent for the homeotropic configuration. The aligning agent was spin coated at the speed of 4000 rev/min for a time of ~100 s. The substrate was kept at a temperature of 80°C for 15 min, then kept at 180°C for a further ~15 min. The substrate was rubbed and then finally kept at 210°C for a further ~15 min prior to its use as one of the windows of the cell. The second window of the cell was treated similarly.

The minor director of the sample was aligned along the easy axis of the windows especially of KBr. The phenyl stretching band (1160 cm^{-1}) was found to be an excellent indicator for both the nematic and the biaxial orderings. For the tetrapode with the asymmetric mesogen (structural formula given in Figure 6, called *A*), the temperature range of the uniaxial and biaxial phases was established through direct observation of the absorbance components A_{XX} and A_{YY}, shown in Figure 7. Two regions of the nematic phase are easily distinguishable: uniaxial, where the two perpendicular absorbance components are equal, and the second biaxial, where A_{XX} starts to exceed A_{YY}. This implies that, on average, the mesogens are tilted along the *X* rather than along the *Y* direction. In order to determine whether branches of the tetrapode are aligned homeotropically, i.e. normal to the substrate or not, the stretching symmetric (~2900 cm^{-1}) and asymmetric (~2800 cm^{-1}) bands were examined. Values of γ could easily be established and were found to be 0° for the symmetric vibration and 90° for the asymmetric vibration for a particular conformation of the molecule. The results give S ($\simeq$0.3), a typical value of S for an orthogonal alignment of the chains as in the SmA phase. Negligible values for D, P, and C were obtained for the chains. These results show that the alignment of the chain was indeed homeotropic. A platelet is formed by the four mesogens in which the mesogens may be tilted but the major axis of the platelet is normal to the substrate. In order to estimate the angle by which the mesogens are tilted in the platelet, we have determined the apparent order parameter of the mesogens. If S_{app} so determined for the homeotropic

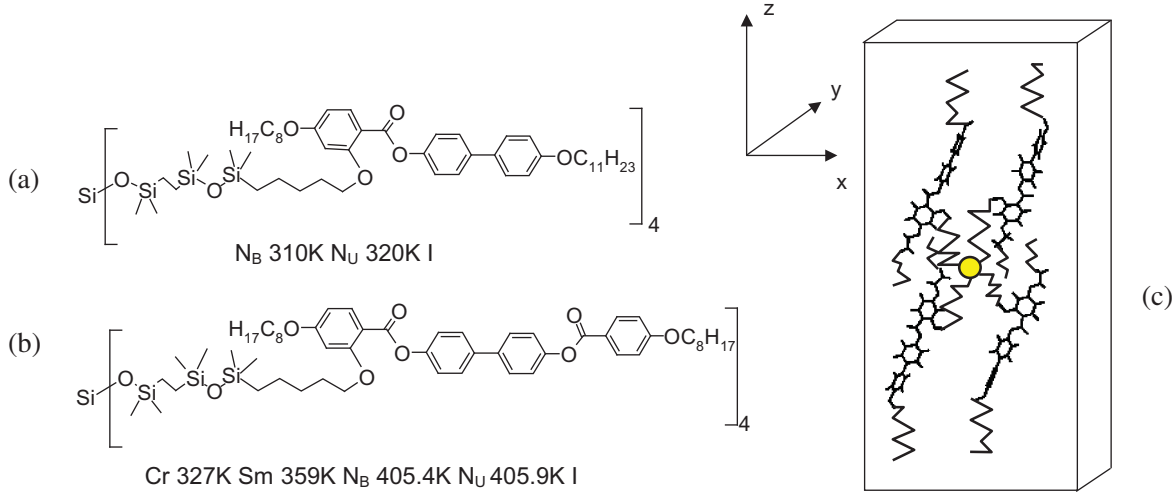

Figure 6. Molecular structure of tetrapodes: (a) *A* and (b) *B* with the asymmetric and symmetric mesogens, respectively. (c) Platelet formed by a molecule of the tetrapode *A* (colour version online).

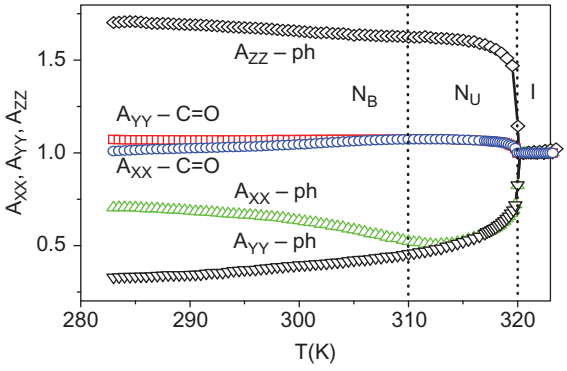

Figure 7. (colour version online). Absorbance components normalised with those of the isotropic phase for A: Δ, A_{XX}; ▽, A_{YY}; ◇, A_{ZZ} values for its phenyl ring stretching band 1160 cm^{-1}, □, A_{YY}; ◇, A_{XX} for the carbonyl 1738 cm^{-1}, A_{XX} and A_{YY} are measured for the homeotropically aligned sample, whereas A_{XX} and A_{ZZ} are measured for the planar homogeneously aligned sample. Figure redrawn, with permission, from Merkel, K.; Kocot, A.; Vij, J.K.; Korlacki, R.; Mehl, G.H.; Meyer, T. *Phys. Rev. Lett.* **2004**, *93*, 237801–1–4. Copyright 2004 by the American Physical Society[1].

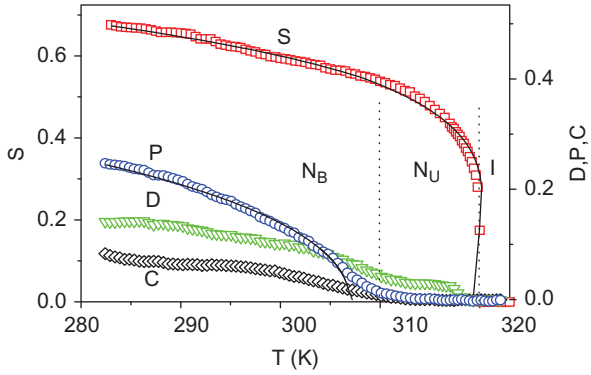

Figure 8. (colour version online). Order parameters for the tetrapode *A*: □, *S*; ○, *P*; ▽, *D*; ◇, *C*, solid line: predicted by the molecular field model of de Gennes. Figure redrawn, with permission from Merkel, K.; Kocot, A.; Vij, J.K.; Korlacki, R.; Mehl, G.H.; Meyer, T. *Phys. Rev. Lett.* **2004**, *93*, 237801–1–4. Copyright 2004 by the American Physical Society[1].

alignment shows unusual temperature dependence for example, it decreases with a reduction in temperature and its value departs significantly from that found for the mesogen with planar configuration, then

$$S_{app} = SP_2(\cos\vartheta), \tag{10}$$

where ϑ is the angle by which the mesogens are tilted and P_2 is the second Legendre polynomial. This is used to calculate ϑ if S is taken from the planar configuration. New coordinates of a particular transition dipole moment within the frame of reference of the platelet are established and a set of four order parameters are recalculated for the platelet. The IR spectra were recorded using a Bio-Rad FTS-6000 spectrometer with a resolution of 1 cm^{-1} and these spectra were averaged over 64 scans. An IR-KRS5 grid polariser was used to polarise the IR beam.

6. Results of the order parameters for the tetrapodes

6.1 *Asymmetrical*

Each mesogen contains three rings, and this compound is termed as the one having asymmetrical mesogens (or an asymmetrical tetrapode). Three components of the IR absorbance, one along and the two perpendicular to the nematic director, were measured for the planar homogeneous and homeotropic sample geometries and shown in Figure 7. At a certain temperature, we observed $A_{XX} > A_{YY}$; this implies that the mesogens on the average are tilted along the X relative to the Y direction. The three absorbance components were converted into the four scalar order parameters of the mesogens (average over the four mesogenic groups) by the procedure described in Section 4. The order parameters for the chains were also calculated, and these indicated that the chains are indeed normal to the substrate. If the mesogens in the homeotropic configuration are tilted by an angle ϑ, the order parameter of the mesogens, S_{app}, is transformed to that for the platelet using Equation (10), results for which are shown in Figure 8.

The observed sequence of phase transitions (see Figure 8) is found to be: at higher temperature there is an isotropic–uniaxial nematic phase transition where both S and D are different from zero; the second transition occurs at a lower temperature, where both P and C are also non-zero. A relatively large value of the phase biaxiality is thus found to be present in a part of the nematic phase of the tetrapode. The schematic diagram of the platelets formed by the tetrapode is shown in Figure 9. The platelets are not shown perfectly ordered along the major director as the order parameter S is considerably less than unity.

6.2 *Results for the tetrapode with the mesogen having a longer core (symmetrical mesogen)*

This tetrapode consists of four rings with an asymmetrical arrangement of the carbonyl bonds as opposed to three previously. This is called the symmetrical tetrapode, and is shown in Figure 6(b). Magnitudes of the absorbances A_{XX} and A_{YY} for the mesogens are such that A_{XX} is larger than A_{YY} but lower than A_{ZZ}. A_{XX} and A_{YY} are the experimentally measured

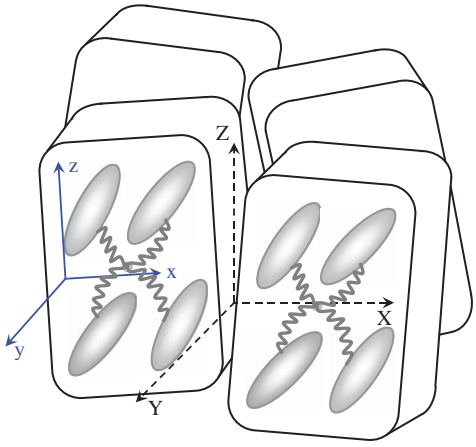

Figure 9. Schematic of the platelets formed by the tetrapode. The molecular system is represented by x, y and z. The mesogens are tilted in the (x–z) plane. Axes X, Y and Z correspond to the laboratory frame. The IR is incident along the Z direction, (X–Y) is the plane of the substrate with X being the rubbing direction. The platelets are not shown perfectly ordered along the major director as the order parameter is considerably less than unity.

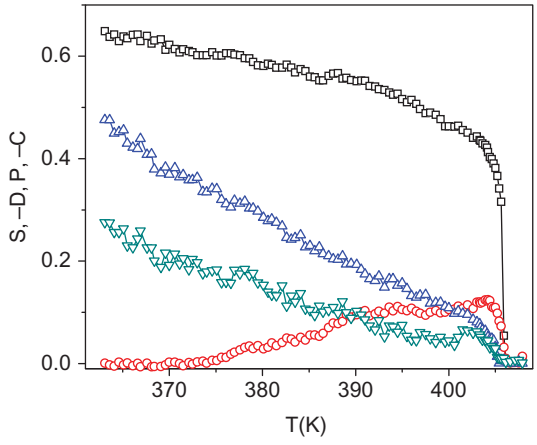

Figure 10. Order parameters of the tetrapode platelet with respect to the frame shown in Figure 11: □, S; ○, - D; △, P and ▽, - C. The mesogenic groups are assumed to be tilted in the x–z plane of the platelet, the y-axis of the platelet is chosen perpendicular to the tilt plane of the platelet (colour version online).

absorbances in the plane of the substrate. A_{ZZ} is the calculated value using Equation (6) and this is found by measuring the total absorbance A_0 with reference to the isotropic phase. The mesogenic groups are tilted by an angle ranging from 30°–37°, with respect to the normal to the substrate, the tilt angle increases with decreasing temperature.

6.3 Tripode

The tripode is built up again of longer mesogenic groups; each of the mesogens has four rings and these are linked to the central benzene ring through an oxygen atom as shown in Figure 11, and the schematic diagram of the platelet is shown in Figure 12.

The order parameters S and D for the terminal chains are calculated and these indicate that the chains are indeed normal to the substrate. They show rather typical values of S, see Figure 13, which confirms the

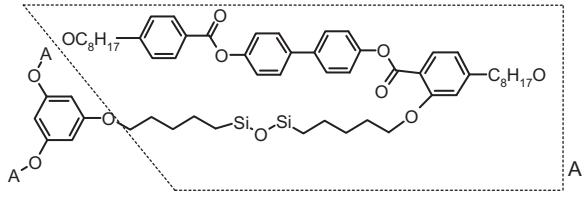

Figure 11. Chemical structure of the tripode with the phase sequence: SmX 310.5 K N 374.6 K I. Each platelet is formed such that the a and c dimensions lying along the x and z directions are of comparable lengths in which the mesogens are tilted and the b dimension along the y direction is much smaller. We choose the director along the z direction, in the plane of the platelet.

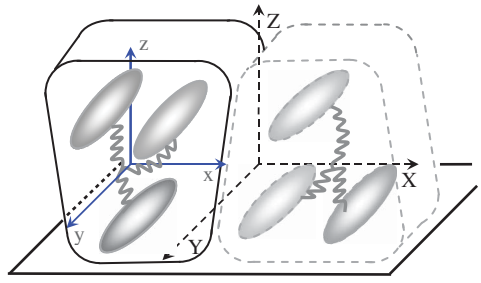

Figure 12. Schematic of the two platelets formed (as an example) by the tripode. The molecular system is represented by x, y and z. Axes X, Y and Z correspond to the laboratory frame. The IR is incident along the Z direction, (X–Y) is the plane of the substrate; X is the rubbing direction. The dotted platelet corresponds to the up/down equivalence (colour version online).

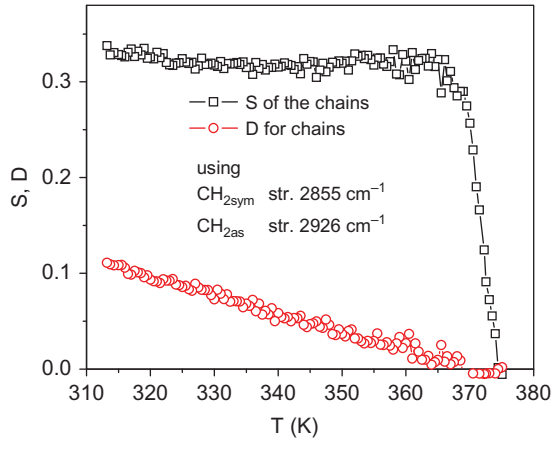

Figure 13. The parameters S and D: □, S; ○, D of the terminal chains of the tripode (colour version online).

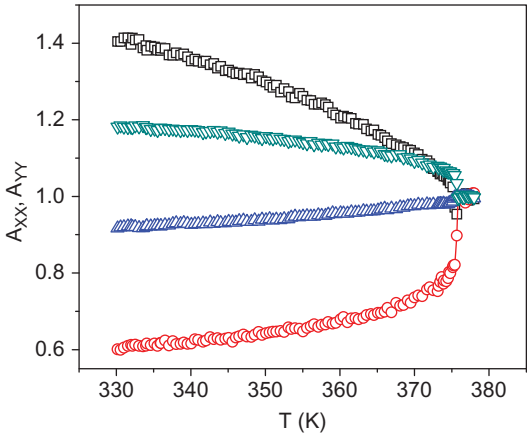

Figure 14. Normalised absorbance components for the mesogens of the tripode scaled with respect to those in the isotropic phase: □, A_{XX}; ○, A_{YY} for 1605 cm^{-1} phenyl stretching band and: Δ, A_{XX}; ▽, A_{YY} for 1738 cm^{-1}, C=O stretching band. A_{XX} and A_{YY} are measured for the homeotropically aligned sample: A_{XX} is the absorbance along the rubbing direction and A_{YY} is normal to it (colour version online).

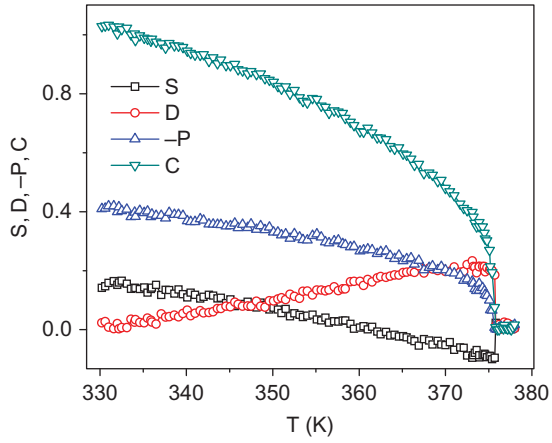

Figure 15. Order parameters of the tripode platelet with respect to the frame shown in Figure 11: □, *S*; ○, *D*; Δ, *-P* and ▽, *C*. Note that *P* is negative. All mesogens are assumed to be tilted in the *x*–*z* plane of the platelet, the *y*-axis of the platelet is chosen perpendicular to the tilt plane of the mesogen (colour version online).

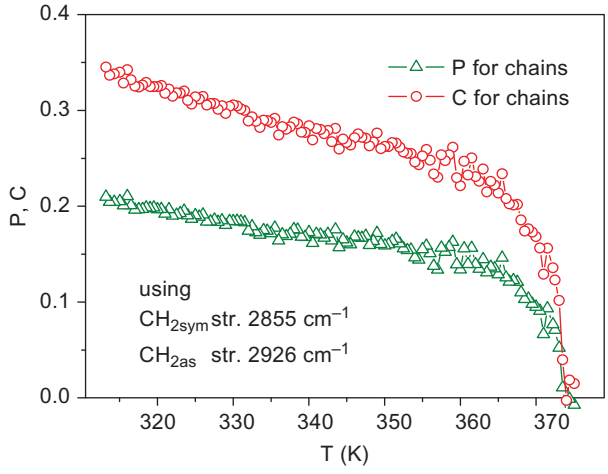

Figure 16. The order parameters *P* and *C* for the chains of the tripode (colour version online).

vertical arrangement, on average, of the terminal chains to the substrate.

The magnitudes of the absorbances A_{XX} and A_{YY} for the mesogens, which are the experimentally measured absorbances in the plane of the substrate, are shown in Figure 14. A_{ZZ} can be calculated using Equation (6) and this is found by measuring the total absorbance, A_0, in reference to the isotropic phase. A_{XX} and A_{ZZ} are comparable but both are larger than A_{YY}. The cores of the mesogenic groups are tilted by an angle of ~55–60° measured with respect to the normal to the substrate.

The results given in Figure 15 appear at first instance to be confusing. The nematic order parameter *S* is very small and is even negative at higher temperatures. This is presumably because of strong fluctuations of the *z*-axis, which is supposed to be the main director. Also, the value of the *C* parameter is much higher than obtained for tetrapode *A*.

The results obtained for terminal chains show quite large values of the phase biaxiality parameters *P* and *C*, see Figure 15. Gorkunov *et al.* [48] have shown that by increasing the tilt of the mesogens (here ~55°), the dimensions *a* and *c* become comparable to each other and both are larger than the dimension *b*. Thus the system may behave rather like a distorted discotic, which is possible if the system is on the other side of the triple point. Gorkunov *et al.* [48] have also shown that the definition of the order parameter is not intrinsically symmetric with respect to the exchange of the molecular axes. They point out that it is essential to select the primary molecular axis, say *z*, and then the two remaining secondary axes are treated in a symmetrical way. We select the *z*-axis as the nematic director as in the uniaxial nematic phase. For the case of rod-like molecules, where the primary axis is that of a biaxial ellipsoid with semi-axes *a*, *b*, *c*, the latter is parallel to the axis *z* if $c > b$ and $c > a$. For the tripode with four mesogen rings, however, the tilt is larger and the frame is altered to a disc-like structure. For the case of a discotic, however, the shortest of the three semi-axes, say again the dimension *c*, is chosen as the *z*-axis. The other two axes lie in the plane of the distorted disc and one of them is slightly larger than the other. The results for the order parameters of the mesogens are converted into that of the frame of the platelet of a disc-like structure.

Also, the symmetry of the experimental results for the absorbance of the stretching phenyl dipole (~1600 cm^{-1}) of the mesogens indicates such a case ($A_{ZZ} \simeq A_{XX} >>$

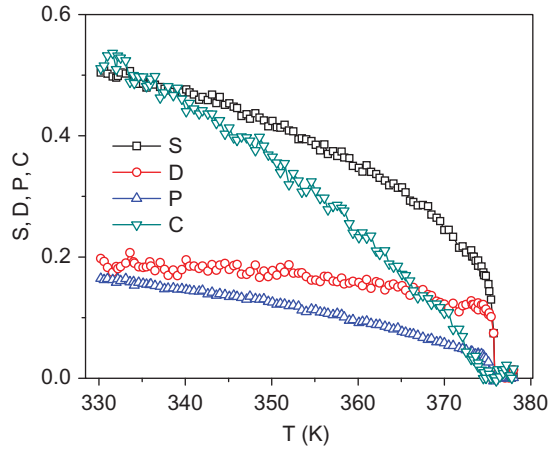

Figure 17. Order parameters for the tripode platelet with a converted frame of reference with reference to that shown in Figure 12 such that ($z \Rightarrow x$, $x \Rightarrow y$, $y \Rightarrow z$): □, S; ○, D; Δ, P and ▽, C. All mesogenic groups are now assumed to be tilted in the x–y plane of the platelet, the z-axis of the platelet is chosen to be normal to the platelet. The transformation equations derived in Gorkunov *et al.* [48] are used to calculate these parameters (colour version online).

A_{YY}). A_{XX} and A_{YY} are the experimentally measured absorbances in the plane of the substrate. A_{ZZ} is the value calculated using Equation (6). A_0 is found by measuring the total absorbance in the isotropic phase. Therefore it is convenient to convert results to another frame, ($z \Rightarrow x$, $x \Rightarrow y$, $y \Rightarrow z$) that reflects the symmetry of the disc-like system (now z is along the smallest dimension), which is a physically meaningful picture. We obtain S, P, D and C as shown in Figure 17 using the formulae derived by Gorkunov *et al.* [48].

7. Relationship between the biaxiality and the order parameters

In this section we wish to connect the scalar order parameters with the refractive index anisotropy. The analysis of nematic biaxiality in terms of the order parameters is based on some of the formulae derived by Song *et al.* [49]. We assume the z-axis of the molecular axis to be the axis of the highest polarisability; the minimum polarisability lies along the x-axis. Then the molecular polarisability tensor is written as

$$\boldsymbol{\alpha}_{\mathrm{mol}} = \begin{pmatrix} \alpha_{xx} & 0 & 0 \\ 0 & \alpha_{yy} & 0 \\ 0 & 0 & \alpha_{zz} \end{pmatrix}. \tag{11}$$

On averaging over the molecular orientations, we can consider that each molecule has, at the centre of its gravity, the effective polarisability tensor

$$\boldsymbol{\alpha} = \begin{pmatrix} \alpha_{XX} & 0 & 0 \\ 0 & \alpha_{YY} & 0 \\ 0 & 0 & \alpha_{ZZ} \end{pmatrix}. \tag{12}$$

The principal values α_{ii} ($i = X, Y, Z$) are given by Dunmur and Toriyama [50]

$$\alpha_{XX} = \bar{\alpha} - \frac{1}{3}\left[\Delta\alpha(S - P) + \Delta\alpha_{\perp}\frac{(D - C)}{2}\right], \tag{13}$$

$$\alpha_{YY} = \bar{\alpha} - \frac{1}{3}\left[\Delta\alpha(S + P) + \Delta\alpha_{\perp}\frac{(D + C)}{2}\right], \tag{14}$$

$$\alpha_{ZZ} = \bar{\alpha} + \frac{2}{3}\left[\Delta\alpha S + \Delta\alpha_{\perp}\frac{D}{2}\right], \tag{15}$$

where $\bar{\alpha}$ is the average polarisability, and $\Delta\alpha$ and $\Delta\alpha_{\perp}$ are the birefringence and the transverse anisotropy of the molecular polarisabilities, respectively. These are given by

$$\begin{aligned} \bar{\alpha} &= (1/3)(\alpha_{xx} + \alpha_{yy} + \alpha_{zz}), \\ \Delta\alpha &= \alpha_{zz} - (1/2)(\alpha_{xx} + \alpha_{yy}), \\ \Delta\alpha_{\perp} &= (\alpha_{xx} - \alpha_{yy}). \end{aligned} \tag{16}$$

We now examine the relationship between the effective polarisability tensor with the principal axes (X, Y, Z) and the dielectric permittivity tensor with principal axes (X', Y' and Z') by considering the local field effect. In general, $X' \neq X$, $Y' \neq Y$, $Z' \neq Z$. In the approximation of the isotropic local field, introduced by Vuks [51],

$$\frac{n_{ii}^2 - 1}{n^2 + 2} = \frac{4\pi N\alpha_{ii}}{3}, \tag{17}$$

where N is the number of molecules per cm^3. $n^2 = (1/3)(n_{XX}^2 + n_{YY}^2 + n_{ZZ}^2)$ is the mean square refractive index. We find

$$n_{XX} - n_{YY} = \frac{4\pi N}{3}\frac{n^2 + 2}{2n_{\perp}}(\alpha_{YY} - \alpha_{XX}), \tag{18}$$

$$n_{XX} - n_{YY} = \frac{4\pi N}{9}\frac{n^2 + 2}{2n_{\perp}}(2\Delta\alpha P + \Delta\alpha_{\perp} C), \tag{19}$$

where

$$n_{\perp} = \frac{n_{XX} + n_{YY}}{2}. \tag{20}$$

Normally, $\Delta\alpha >> \Delta\alpha_{\perp}$, by a factor of at least 10. Equation (19) shows that if $P \simeq 0$, then the refractive index anisotropy comes mainly from C, the biasing of rotations along the long molecular axes. On knowing

$\Delta\alpha_\perp$ and $n_\perp$, we can determine the biaxiality$(n_X - n_Y)$. P can be positive or negative, depending on the relative fluctuations of the long molecular axes along the X and Y directions. However, C is generally positive. This can be negative for some compounds in the SmC* phase [49], where the shortest axis of polarisability is normal to the tilt plane. In most compounds, the shortest axis of polarisability lies in the tilt plane. It should be noted that Equation (19) for the phase biaxiality is not explicitly dependent on the parameter D, but D contributes to C, which is explicitly included in the expression for the biaxiality in the refractive index.

8. Discussion of the order parameters

We find that the orientational order parameter S is discontinuous for the tetrapode A at the I–N_U transition, confirming the first-order transition. The molecular biaxiality parameter D is small but finite in the N_U phase. At the N_U to N_B transition, the biaxial order parameters P and C increase rather continuously, indicative of the second-order N_U–N_B transition. P increases to ~0.35, whereas C increases only to ~0.1. The surprising aspect of our results for the tetrapode having asymmetrical mesogens is that C is much smaller than either P or D. For a perfect nematic ordering, i.e., for $S \rightarrow 1$, Sonnet *et al.* [52] predict that C based on its definition should be $C \rightarrow 3$ and $P \approx 0.1$ as P is a measure of the difference in the fluctuations of the long molecular axis in the X–Y and Y–Z planes. The discrepancy in the predicted and experimental results shows that the system is not close to the perfect nematic ordering. The packing of these tetrapodes may be such that P stays higher than calculated theoretically in the temperature range of experimental investigations. The interaction parameter controlling the rotation of the short axes is likely to be very small. This implies that in many molecular systems fluctuations are larger than the entropic and other considerations that keep the minor director staying completely aligned. The main reason for an unambiguous observation of a biaxial nematic phase in the literature may lie in the fact that the ordering of the short axes as shown in Figure 1(a) is not perfect, and the fluctuations arising from thermal energy alone are large enough to disturb the perfect biaxial ordering, thus preventing the biaxial structure being maintained over the time period of investigations in a number of systems.

9. Testing of the mean field model of de Gennes for biaxial nematics

Since the absolute values of the order parameters have been determined, the mean field model of de Gennes [3] for a biaxial phase can easily be tested. The free energy density, as a function of the second, δ, and third, Δ, fundamental invariants of the order tensors of the system [3] is given as

$$F = \frac{a}{2}\delta + \frac{b}{3}\Delta + \frac{c}{4}\delta^2 + \frac{d}{5}\delta\,\Delta + \frac{e}{6}\Delta^2 + \frac{e'}{6}\delta^3 \quad +---, \tag{21}$$

where $\delta = (3S^2 + P^2)/2$ and $\Delta = 3S(S^2 - P^2)/4$. In the simplest form of the model, a is assumed to be a linear function of temperature, $a = \alpha(T - T^*)$, and furthermore b and the higher order coefficients are essentially independent of temperature. The minimisation of F with respect to the invariants gives the critical temperature T^*. For the phase to be biaxial, the condition $\delta^3 \neq 6\Delta^2$ must be satisfied. From Figure 8 in Section 5, the temperature dependencies of the invariants δ and Δ are clearly found to be non-linear, which signify the importance of the δ^3 term in F. Only five factors, c/α, d/α, e'/α, b/e, and d/e, are varied when fitting the model to the data. Figure 18 shows that S and P are reproduced extremely well by the model (except for a narrow range of temperatures at the I–N transition due to a weak first-order transition). The fitting shows that the results can be described by the mean field model of de Gennes for a biaxial nematic phase, where the cubic term in the free energy given by Equation (21) is also important.

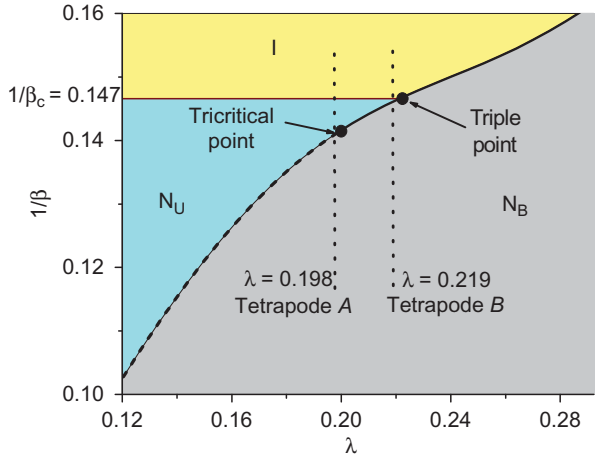

Figure 18. (colour version online). Plot of reduced temperature ($1/\beta$) versus the shape anisotropy λ. This is calculated as 0.198 and 0.219 for the tetrapodes based on their dimensions. The triple point defines the coexistence of the three phases I, N_U and N_B. The tricritical point is different from the triple point by the range of values of λ that determine where the first-order N_U to N_B meet with the second-order N_U to N_B transitions. Figure redrawn, with permission from Merkel, K.; Kocot, A.; Vij, J.K.; Korlacki, R.; Mehl, G.H.; Meyer, T. *Phys. Rev. Lett.* **2004**, *93*, 237801–1–4. Copyright 2004 by the American Physical Society[1].

The phase diagram for the tetrapode can be interpreted in terms of the molecular-field model of Sonnet *et al*. [52], which employs a shape anisotropy λ of the biaxial dielectric susceptibility, and the reduced temperature $1/\beta$ ($\beta = U_0/k_BT$, where U_0 is the molecular interaction energy). In the $((\lambda,\ 1/\beta))$ plane, a sequence of phases dependent on λ is shown in Figure 18, where the solid and broken lines represent the first- and second-order phase transitions, respectively. The point where the line for the first-order N_U to N_B meets with that for the second-order N_U to N_B is called the tricritical point. For the given phase diagram, in the $(\lambda, 1/\beta)$ plane, the tricritical point occurs when $\beta_t = 7.07$. The same sequence of phases occurs until $\lambda = \lambda_c \simeq 0.22$ and for $\lambda > \lambda_c$, a first-order direct transition from I–N_B is observed without an intermediate N_U phase. The experimental values of the transition temperatures for both tetrapodes are shown on the plot. We assign molecular interaction energies, U_0, of 3.01×10^{-20} J and 3.83×10^{-20} J for tetrapodes *A* and *B* in order to obtain the I–N transition temperatures in reduced units; $1/\beta_c = 0.147$ as in the model. If we use these scaling factors for the N_U–N_B transition, we obtain $1/\beta_c$ of 0.128 and 0.14 for tetrapodes *A* and *B*, respectively. The corresponding values of λ can be read from the abscissa of the plot shown in Figure 18 as their N_U–N_B transition. These are 0.198 and 0.219 for tetrapodes *A* and *B*. The shape anisotropy factor λ, using its definition, is estimated from the basic dimensions of the platelet. λ is calculated to be 0.18 and 0.22 for *A* and *B*, and these values agree reasonably with those obtained from the phase diagram. For tetrapode *A*, the N_U–N_B transition appears to be second order and is close to the triple point. Thus the model is able to reasonably predict the appearance of the biaxial phase, its stability, and the nature of the phase transitions for both tetrapodes. This analysis is to be extended to the tripode.

Acknowledgements

The authors thank K. Merkel and M. Nagaraj for simulation of the structure and some of the experimental work given. We thank G.H. Mehl of the University of Hull for having given us the compounds. G.R. Luckhurst, D. Photinos, M. Gorkunov, Jang-Kun Song, A. Fukuda and M.A. Osipov are thanked for discussions. This work was partially funded by EU Bind Project No FP7, SFI RFP 06/ENE039 and SFI 07/W.1/I1833. A.K. acknowledges PMSIT - grant N202 282734.

Note

References

[1] Maier, W.; Saupe, A. *Z. Naturforsch*, **1959**, *14a*, 882.
[2] Bisi, F.; Luckhurst, G.R.; Virga, E.G. *Phys. Rev. E: Stat., Nonlinear, Soft Matter Phys.* **2008**, *78*, 021710-1-6.
[3] de Gennes, P.G.; Prost, J. *The Physics of Liquid Crystals*, 2nd ed.; Oxford Science Publications: New York, 1993.
[4] Freiser, M.J. *Phys. Rev. Lett.* **1970**, *24*, 1041–1043.
[5] Straley, J.P. *Phys. Rev. A: At., Mol., Opt. Phys.* **1974**, *10*, 1881–1887.
[6] Yu, L.I.; Saupe, A. *Phys. Rev. Lett.* **1980**, *45*, 1000–1003.
[7] Luckhurst, G.R.; Romano, S. *Mol. Phys*. **1980**, *40*, 129–139.
[8] Malthête, J.; Nguyen, H.T.; Levlut, A.M. *J. Chem. Soc. Chem. Commun.* **1986**, 1548–1549.
[9] Chandrasekhar, S.; Ratna, B.R.; Sadashiva, B.K.; Raja, V.N. *Mol. Cryst. Liq. Cryst.* **1988**, *165*, 123–130.
[10] Leube, H.F.; Finkelmann, H. *Makromol. Chemie* **1991**, *192*, 1317–1328.
[11] Li, J.-F.; Percec, V.; Rosenblatt, C.; Lavrentovich, O.D. *Europhys. Lett.* **1994**, *25*, 199.
[12] Vanakaras, A.G.; Photinos, D.J. *Mol. Cryst. Liq. Cryst.* **1997**, *299*, 65–71.
[13] Longa, L.; Stelzer, J.; Dunmur, D. *J. Chem. Phys*. **1998**, *109*, 1555–1566.
[14] Chiccoli, C.; Feruli, I.; Lavrentovich, O.D.; Pasini, P.; Shiyanovskii, S.V.; Zannoni, C. *Phys. Rev. E: Stat., Nonlinear, Soft Matter Phys.* **2002**, *66*, 030701 (R).
[15] Luckhurst, G.R. *Thin Solid Films* **2001**, *393*, 40–52.
[16] Praefcke, K. *Braz. J. Phys.* **2002**, *32*, 564–569.
[17] Pratiba, R.; Madhusudana, N.V.; Sadashiva, B.K. *Science* **2000**, *288*, 2184–2187.
[18] Eremin, A.; Diele, S.; Pelzl, G.; Nadasi, H.; Weissflog, W.; Salfetnikova, J.; Kresse, H. *Phys. Rev. E: Stat., Nonlinear, Soft Matter Phys.* **2001**, *64*, 051707-1-6; Keith, C.; Prehm, M.; Panarin, Y.P.; Vij, J.K.; Tschierske, C. *Chem. Comm*. **2010**, *46*, 3702–3704.
[19] Shimbo, Y.; Gorecka, E.; Pociecha, D.; Araoka, F.; Goto, M.; Takanishi, Y.; Ishikawa, K.; Mieczkowski, J.; Gomola, K.; Takezoe, H. *Phys. Rev. Lett.* **2006**, *97*, 113901-1-4.
[20] Madsen, L.A.; Dingemans, T.J.; Nakata, M.; Samulski, E.T. *Phys. Rev. Lett.* **2004**, *92*, 15505-1-4.
[21] Luckhurst, G.R. *Nature (London, UK)* **2004**, *430*, 413.
[22] Acharya, B.R.; Primark, A.; Kumar, S. *Phys. Rev. Lett.* **2004**, *92*, 145506-1-4.
[23] Luckhurst, G.R. *Agnew Chem. Int. Ed.* **2005**, *44*, 2834–2836.
[24] Severing, K.; Saalwachter, K. *Phys. Rev. Lett*. **2004**, *92*, 125501-1-4.
[25] Merkel, K.; Kocot, A.; Vij, J.K.; Korlacki, R.; Mehl, G.H.; Meyer, T. *Phys. Rev. Lett.* **2004**, *93*, 237801-1-4.
[26] Figureirinhas, J.L.; Cruz, C.; Filip, D.; Feio, G.; Ribeiro, A.C.; Frère, Y.; Meyer, T.; Mehl, G.H. *Phys. Rev. Lett.* **2005**, *94*, 107802-1-4.
[27] Filip, D.; Cruz, C.; Sebastião, P.J.; Robeiro, A.C.; Vilfan, A.C.; Meyer, T.; Kouwer, P.H.J.; Mehl, G.H. *Phys. Rev. E: Stat., Nonlinear, Soft Matter Phys.* **2007**, *75*, 011704-1-11.

[28] Nepune, F.; Kang, S.W.; Sharma, S.; Carney, D.; Meyer, T.; Mehl, G.H.; Allender, D.W.; Kumar, S.; Sprunt, S. *Phys. Rev. Lett.* **2006**, *97*, 207802-1-4.
[29] Berardi, R.; Muccoli, L.; Orlo, S.; Ricci, M.; Zannoni, C. *J. Phys. Cond. Matt.* **2008**, *20*, 463101-1-16.
[30] Coffey, W.T.; Kalmykov, Y.P.; Quari, B.; Titov, S.V. *Physica A* **2006**, *368*, 362–376.
[31] Martin, A.J.; Meier, G.; Saupe, A. *Symp. Faraday Soc.* **1971**, *5*, 119–133.
[32] Southern, A.D.; Brimicombe, P.D.; Siemianowski, S.D.; Jaradat, S.; Roberts, N.; Görtz, V.; Goodby, J.W.; Gleeson, H.F. *Europhysics Lett.* **2008**, *82*, 56001-1-6. See also the review article by Gleeson, H.F.; Southern, C.D.; Brimicombe, P.D.; Goodby, J.W.; Görtz, V. *Liq. Cryst*. **2010**, *37*, 949–959.
[33] Dunmur, D.A., Toriyama, H. In *Handbook of Liquid Crystals*: Demus, D., Goodby, J., Gray, G.W., Spiess, H.-W., Vill, V., Eds.; Wiley-VCH: Weinheim, 1998; Vol. 1, Ch. VII.1, p 189.
[34] Emsley, J.W. In *Nuclear Magnetic Resonance of Liquid Crystals*: Emsley, J.W., Ed.; Reidel: Dordrecht, 1983; p 379.
[35] Zannoni, C. In *The Molecular Dynamics of Liquid Crystals*: Luckhurst, G.R., Veracini, C.A., Eds.; Kluwer: Dordrecht, 1994; p 34.
[36] Scaife, B.K.P.; Vij, J.K. *J. Chem. Phys.* **2005**, *122*, 174901-1-11.
[37] Neff, V.D.; Gulrich, L.W.; Brown, G.H. In *Liquid Crystals*; Brown, G.H., Dienes, G.D., Labes, M.M., Eds.; Gordon Brown: New York, 1967; pp 21–25.
[38] Maier, W.; Saupe, A. *Z. Naturforsch* **1961**, *16a*, 816.
[39] Turrell, G. *Infrared Raman Spectra of Crystals*; Academic: New York, 1972; pp 153–158.
[40] Kruk, G.; Kocot, A.; Wrzalik, R.; Vij, J.K.; Karthaus, O.; Ringsdorf, H. *Liq. Cryst.* **1993**, *14*, 807–819.
[41] Vij, J.K.; Kocot, A.; Perova, T.S. *Mol. Cryst. Liq. Cryst*. **2003**, *397*, 531–544.
[42] Kocot, A.; Vij, J.K.; Perova, T.S. In *Advances in Liquid Crystals: A Special Volume of Advances in Chemical Physics*: Vij, J.K., Ed.; Prigogine, I., Rice, S.A., Series Eds.; Wiley: New York, 2000; Vol. 113, p 203.
[43] Hild, E.; Kocot, A.; Vij, J.K.; Zentel, R. *Liq. Cryst.* **1994**, *16*, 783–803.
[44] Merkel, K.; Kocot, A.; Vij, J.K.; Mehl, G.H.; Meyer, T. *J. Chem. Phys*. **2004**, *121*, 5012–5021.
[45] Ossowska-Chrusciel, M.D.; Korlacki, R.; Kocot, A.; Chruściel, J.; Zalewski, S. *Phys. Rev. E: Stat., Nonlinear, Soft Matter Phys.* **2004**, *70*, 041705-1-10.
[46] Peroukidis, S.D.; Karahaliou, P.; Vanakaras, A.G.; Photinos, D.J. *Liq. Cryst.* **2009**, *36*, 727–737.
[47] Kocot, A.; Wrzalik, R.; Vij, J.K. *Liq. Cryst.* **1996**, *21*, 147–151.
[48] Gorkunov, M.V.; Osipov, M.A.; Kocot, A.; Vij, J.K. *Phys. Rev. E: Stat., Nonlinear, Soft Matter Phys.* **2010**, *81*, 061702-1-10.
[49] Song, J.K.; Chandani, A.D.L.; Fukuda, A.; Vij, J.K.; Kobayashi, I.; Emelyanenko, A.V. *Phys. Rev. E: Stat., Nonlinear, Soft Matter Phys.* **2007**, *76*, 011709-1-13.
[50] Dunmur, D.A.; Toriyama, H. In *Handbook of Liquid Crystals*: Demus, D., Goodby, J., Gray, G.W., Spiess, H.-W., Vill, V., Eds.; Wiley-VCH: Weinheim, 1998; Vol. 1, Ch. VII.3, p 215.
[51] Vuks, M.F. *Opt. Spektrosk.* **1966**, *20*, 644.
[52] Sonnet, A.M.; Virga, E.G.; Durand, G.E. *Phys. Rev. E: Stat., Nonlinear, Soft Matter Phys.* **2003**, *67*, 061701-1-7.